

Doppler Global Velocimetry Measurements of Supersonic Flow Fields

James F. Meyers
NASA Langley Research Center
Hampton, Virginia 23681, USA

Introduction

The application of Doppler Global Velocimetry (DGV) to high-speed flows has its origins in the original development of the technology by Komine *et al* (1991). Komine used a small shop-air driven nozzle to generate a 200 m/s flow. This flow velocity was chosen since it produced a fairly large Doppler shift in the scattered light, resulting in a significant transmission loss as the light passed through the Iodine vapor. This proof-of-concept investigation showed that the technology was capable of measuring flow velocity within a measurement plane defined by a single-frequency laser light sheet. The effort also proved that velocity measurements could be made without resolving individual seed particles as required by other techniques such as Fringe-Type Laser Velocimetry and Particle Image Velocimetry.

The promise of making planar velocity measurements with the possibility of using 0.1-micron condensation particles for seeding, Dibble *et al* (1989), resulted in the investigation of supersonic jet flow fields, Elliott *et al* (1993) and Smith and Northam (1995) – Mach 2.0 and 1.9 respectively. Meyers (1993) conducted a wind tunnel investigation above an inclined flat plate at Mach 2.5 and above a delta wing at Mach 2.8 and 4.6. Although these measurements were crude from an accuracy viewpoint, they did prove that the technology could be used to study supersonic flows using condensation as the scattering medium. Since then several research groups have studied the technology and developed solutions and methodologies to overcome most of the measurement accuracy limitations:

DLR – Köln (Roehle and Schodl (1994, 1997), and Roehle (1999)),
NASA Ames Research Center (McKenzie (1996, 1997), and McKenzie and Reinath (2000)),
NASA Langley Research Center (Meyers (1995, 1996), Meyers and Lee (1999), Meyers *et al* (1998, 2001), Smith (1998), and Smith *et al* 1996)),
Ohio State University (Clancy *et al* (1996, 1998), and Samimy and Wernet (2000)),
Princeton University (Forkey *et al* (1995)),
Rutgers University (Elliott and Beutner (1999), and Elliott *et al* (1993, 2000)),
and
West Virginia University (Naylor and Kuhlman (1998)).

These methods include:

- Laser Frequency Monitor – Measure the laser output frequency for each video frame to account for laser frequency drift,
- Active feedback laser frequency control – Minimize laser frequency drift,
- Vapor-limited Iodine cells – Stable optical transmission characteristics,
- Low noise cameras – Minimize electronic noise, and image integration capability,
- Iodine absorption line calibration with a rotating wheel – Increased measurement accuracy,
- Background light removal – Eliminate all collected light not originating from the laser light sheet,
- Image dewarping – Removes all perspective and optical distortions from the images along with matching optical magnification and orientations of the six data images,
- Intensity Flat Field – Determines and corrects the spatial variation of signal-to-reference ratios independent of optical frequency,
- Frequency Flat Field – Determines and corrects the spatial variation of optical frequency originating from crystal-based lasers, and
- Integrate images – Minimizes division noise at the edge of a meandering smoke plume.

Using the above components and techniques, a DGV system may be constructed for supersonic applications with better accuracy than previously reported. However, is this the best that can be done?

Iodine Vapor Cell Calibration

The expected Doppler shift in a supersonic flow may be hundreds of MHz. This becomes a problem if three-component measurements are desired since one of the components will yield a Doppler shift of the opposite sign, leading to a difference in Doppler frequencies that is greater than the frequency span of the Iodine absorption line edge. The needed frequency range has been obtained by using a buffer gas, e.g., nitrogen, within the cell to decrease the slope, Elliott *et al* (1997), and by using both sides of the absorption line, Meyers (1993). Although these techniques will provide measurements, their accuracy is compromised. If a buffer gas is used, the absorption line ceases to remain linear and the velocity resolution decreases. Using both sides of the absorption line would provide linear measurement ranges, however it requires an accurate measure of the frequency span at the bottom of the absorption line. Although measurements of Doppler frequency from a rotating wheel provide very accurate calibrations, figure 1, (Meyers *et al* (2001)), the dynamic range is insufficient to span the bottom of the line.

Of the two approaches, using the total absorption line would provide more accurate measurements if the dynamic range of the calibration technique could be improved. New advances in Acoustic Optic Frequency Shifters (AOFS) or Bragg Cells have provided a solution. Cells constructed of Tellurium Dioxide (TeO_2) crystals can provide a frequency shift of 270 MHz with a tunable bandwidth of 140 MHz. A double pass optical system can be constructed, figure 2, to double the frequency shift and bandwidth while maintaining optical alignment as the drive frequency is scanned. Employing the overlapping segment method of calibration used with the rotating wheel and the increased bandwidth capabilities of the AOFS, the entire absorption line can be accurately calibrated, figure 3, (Lee and Meyers (2005)).

The AOFS system can also be applied to a DGV optical system to allow the laser frequency to be tuned to the minimum transmission point of the absorption line. The feedback control laser beam frequency would be shifted with the AOFS into the linear region to maintain stability of the active feedback network used to minimize laser frequency drift. This would place the collected scattered light frequencies within the linear region on both sides of the absorption line. Additionally, any laser light scattered from surfaces collected by the receivers would be attenuated by the Iodine vapor.

Fiber-Optic Based DGV System

Typically supersonic wind tunnels have two high-quality windows on opposite sides of the test section to provide optical access for Schlieren optical systems. Other windows, if they exist, are usually lower in quality and fairly small. Normally wind tunnel investigations are concerned with the flow field passing around an aerodynamic model. This necessitates that the three receivers be mounted on one side of the tunnel to avoid optical blockage of the flow field by the model. The photograph of a three-component system mounted in the Langley Unitary Plan Wind Tunnel (UPWT) illustrates the difficulties of system installation in a supersonic wind tunnel, figure 4. Nobes *et al* (2002) developed a DGV system using fiber-optic bundles to collect and transmit scattered light from three locations to a single DGV receiver system. The success of this effort indicates that a fiber-optic based system would ease the installation and usability of DGV for supersonic wind tunnel applications.

The fiber optic bundles used by Nobes *et al* (2002) and Willert *et al* (2003) were custom units with four viewing fibers that merged into a single bundle that could be viewed using image transfer optics by a single DGV receiver. Each of the viewing fiber bundles consisted of 200k individual fibers arranged in a 4-x 5-mm rectangular pattern. Three of the 4.5 m-long fiber bundles were equipped with C-mount lenses to image the laser light sheet from three viewing directions. The fourth bundle was used to transmit a portion of the laser beam to monitor the laser frequency. The bundles produced high quality images of laboratory experiments (Nobes *et al* (2002))

and high-speed cryogenic flows (Willert *et al* (2003)). Although the size of these bundles provides good image quality, their large bending radius prohibits their use in small spaces and they are susceptible to fiber breakage leaving holes in the viewed image.

The approach chosen at NASA Langley was to use individual 0.5-mm diameter fiber bundles, containing 30k fibers, as a potential system configuration for internal flow applications in engine inlets. Since each bundle is a separate entity, the needed lengths may be selected for each application. A screw-on mount was used to interface a 4-mm lens at the viewing end of each fiber bundle and the opposite end of the bundle was sheathed with a 10-cm long stainless steel tube with a wall thickness of 0.1-mm. The three bundles were grouped together with their images being transferred to the DGV cameras through a series of lenses, figure 5. The image quality was acceptable, but the small collecting lens limited the modulation transfer function, figure 6. No fiber breakage has occurred in almost two years of laboratory and wind tunnel usage. The laser frequency was monitored by transmitting a portion of the laser beam through a multimode fiber to the lenses that imaged the component fiber bundles.

The flexibility of the fiber-optic based system led to its selection as the approach to investigate supersonic flow fields about models in the Langley UPWT. The simplicity of the fiber-optic based system, figure 7, is easily seen when compared with the previous free-space system shown in figure 4. In addition, the common viewing area was increased from 250-x 250-mm area fixed at the center of the test section – free space system (Meyers (1993)), to a 350-x 350-mm area that may be located anywhere within the test section – fiber-optic based system.

Modifications to Calibration / Correction Procedures

The use of a fiber-optic based DGV system for supersonic flow field applications has necessitated the addition to and/or modification of a few of the calibration / correction procedures outlined above. They include the addition of an alignment procedure to insure that the fiber has not rotated the acquired image, and the development of a “virtual” registration target to account for minor differences in the planes defined by the alignment registration target and light sheet, respectively. The method for determining the Intensity Flat Field was modified to simplify its acquisition and reduce needed tunnel run time.

Fiber-Optic Rotation. - When a DGV receiver system is installed about a wind tunnel test section, its optical plane is typically horizontal with the optical axis panned/tilted to view the center of the laser light sheet. When fiber-optic bundles are used, the optical plane can be easily rotated along the length of the fiber. This rotation can result in significant errors in the measurement of the velocity vector if the registration target image characteristics are used to determine the viewing location.

For example, testing has shown this to be approximately ± 35 m/s for a rotation of ± 8 -degrees. The straightforward solution is to manually measure the location of the center of the registration target along with the three viewing locations. However, errors will occur because of the inability to accurately account for windows, mirrors, etc. used to view the measurement plane. Rotating the registration target in pan and tilt to align the center of the target with the optical axis of the viewing fiber using a laser aligned perpendicular to and centered in the target will provide an orthogonal grid for the collecting lens, figure 8. If the acquired camera image is not orthogonal, the fiber can be rotated to the correct orientation.

Virtual Registration target. - Although great care may be taken to insure that the dewarping calibration target is placed in the light sheet plane, minor differences may still occur. These differences may arise from millimeter out of plane settings along the length of the registration target, registration target bending, distortions in tunnel windows at wind-on conditions, thickness of the light sheet as compared to the registration target, etc. If a particle generator is used to illuminate the light sheet in a manner to produce intensity structures, the three reference camera images can be piecewise cross-correlated to produce new alignment positions for two of the images as compared to the layout of the third. Thus the dewarping process would then consist of two parts – dewarping each image based on the physical registration target, then dewarping the two component images based on the new alignment positions obtained from the piecewise cross correlation offsets. This procedure has been shown to reduce velocity biases of up to 5-percent based on freestream measurements at Mach 2.

Intensity Flat Field. - The Intensity Flat Field is routinely obtained by adjusting the laser frequency to be outside the absorption line and freestream data images acquired under test run conditions. This produces correction images that account for the illumination ratio generated by the DGV receiver beamsplitter based on the polarization characteristics of the seeding particles in the flow, along with any spatial variations in transmissivity through the optical system. The large Doppler shifts from supersonic flows make this approach impractical. The laser frequency must be adjusted to move each Doppler shifted component frequency outside the absorption line individually to insure that a component frequency has not moved into an adjacent absorption line. An alternative approach would be to determine the Intensity Flat Field without flow using a humidifier to generate a water particle cloud. This has the advantage of keeping all scattered light frequencies the same as the laser frequency – therefore only one laser tuning is needed. However, the particles will not have the same size distribution as condensation, thus the polarization effects are different. Also, optical effects from tunnel window bending as the tunnel pressure falls to test conditions would not be determined. A second “Intensity” Flat Field would then be required. With the tunnel set to normal operating conditions and the model located downstream of the measurement plane, freestream velocity measurements can be obtained. With an assumption that the

freestream flow direction is constant and known, freestream measurements can be converted into a second Intensity Flat Field to account for the optical and polarization effects under wind-on conditions. Once determined, both Flat Fields are applied without modification for the duration of the run.

Flow Field Investigation at Mach 2

The shedding of foam from the space shuttle external tank that impacted the wing leading edge of the Columbia raised concern about the effect of shocks from the Solid Rocket Booster (SRB) on the surface of the external tank. In order to obtain a better understanding of this interaction, a model was constructed to simulate the fundamental flow field. The model consisted of a large flat plate to simulate the external tank, and an attached cylinder with an ellipsoidal nose to simulate the SRB, figure 9. The three-component, fiber-optic based DGV system was used to investigate the flow field by measuring a series of cross-flow planes as the model was traversed upstream in a Mach 2 flow. A single injection of 3 liters of water in the wind tunnel provided the condensation needed for a day's run.

The first investigation was to measure the bow shock downstream of the plate leading edge at -3° and 0° angle of attack at several stations downstream from the leading edge. This investigation would serve as a confidence builder in the accuracy and resolution of the fiber-optic based system. The results are shown in figure 10. At -3° angle of attack, the axial velocity decreased and the vertical velocity increased by approximately 15 m/s behind the shock (freestream = 510 m/s). These velocities remained constant from the shock to the flow boundary layer. At 0° angle of attack, the same 15 m/s change was observed, but the flow velocity returned to freestream levels behind the shock. The velocity maps presented in figure 10 represent an on-camera integration of 0.5 seconds along with a frame-to-frame integration of the 50 data frames acquired at each axial position. The temporal statistics were determined by computing the flow field for each of the 50 frames and calculating the standard deviation about the mean along the center vertical profile. The results of this calculation for figure 10 (e) at 0° angle of attack are presented in figure 11. The standard deviation for components A, B and C are less than 2 m/s rising at the extremes from model flare (near surface) to errors from extrapolated optical alignment (127-mm extrapolation from the registration target data). The conversion from DGV components to orthogonal components increased the standard deviations up to 2 m/s for streamwise (U) and crossflow (V) and 7 m/s for vertical (W). Spatial consistency was tested by computing the statistics for the orthogonal components for all pixels viewing the area above the shock, outlined by the rectangle in figure 12. As seen in the figure, the histogram was Gaussian in nature with very small standard deviations:

| Component | Mean (m/s) | Standard Deviation (m/s) |
|-----------|------------|--------------------------|
| U | 510.6 | 1.03 |
| V | -0.9 | 0.64 |
| W | 0.5 | 2.40 |

The larger standard deviation in W for both the temporal and spatial statistics was expected, as the trigonometric errors for W are large since the flat plate limited the viewing positions to the upper half of the test section.

As the model was moved further upstream, the shock from the attached store was found. A few example flow field planes are shown in figure 13. The expansion of the shock is clearly seen along with the crossflow entering and leaving the shock region. In this case not only does the axial flow decrease velocity within the shock, it accelerates slightly above freestream behind the shock. The total velocity variation is less than 30 m/s for a freestream velocity of 510 m/s. It is noted that the missing flow regions on the left of the image are caused by the presence of the store and flare from the store as the light sheet impinges on the model. Regions near this area should not be considered accurate as they are influenced by secondary scattered light from the flat-black painted model (Roehle (1999)).

An attempt to use the fiber-optic based DGV system to measure the boundary layer velocity profile was also conducted. As seen in figures 10 and 13, flare from the flat-black painted flat plate was sufficient to prohibit measurements near the surface, even with a nearly parallel light sheet. Thus a different approach was attempted. The primary laser beam was diverted from the light sheet forming optics to a multimode optical fiber that transmitted a laser beam vertically from inside the flat plate model, figure 14. Even with an angle of attack setting of 0-degrees, the flat plate model deflected at run conditions causing the laser beam to deviate from the measurement plane. Although this deflection prohibited the dewarping procedures from aligning the beam among the three components, it was still possible to resolve the individual DGV components. The velocity profile was found to have the same characteristics as the light sheet measurements within the main flow. As the surface was approached, a distinct change in slope was found in all three components indicating the entry into the boundary layer. Once the surface was reached, the profile reverses as the scattered light from the laser beam was reflected by the model surface. Even though orthogonal components could not be accurately determined because of the model movement, the calculations were performed and the results compared with the corresponding profile from the light sheet data, figure 15. Although the levels are approximately the same, the out-of-plane effects from the beam deflection clearly show a tracking between the V and W components resulting from the model movement.

This demonstration flow field investigation served a second purpose of determining if DGV could be used in a production mode to quickly measure the flow at a series of

axial stations. The data acquisition time for each station was 25 seconds (50 frames) with an additional 15 seconds needed to write the data to disk. Sample data processing to yield three component plots, as shown in figures 10 and 13, required 40 seconds per plane. In total, the production demonstration included the acquisition of image data at 43 axial stations; redirecting the laser beam to the embedded fiber and obtaining the boundary layer profile; and, returning the laser beam to the light sheet optics to acquire a repeat freestream measurement after the model was moved downstream to clear the light sheet. These tasks were completed within 90 minutes of tunnel run time. On average, approximately half of the time was required for data acquisition and storage, and the remaining time needed to move the model.

Summary

A demonstration Mach 2-flow field investigation using a fiber-optic based Doppler Global Velocimeter has been described. The objective was to determine if the shock wave flow pattern about a simulated shuttle SRB/external tank could be mapped using DGV technology. A secondary goal was to determine if the technology could be configured to measure the flow boundary layer. The results presented confirm that these objectives were realized. The system was also capable of being utilized under production mode conditions, producing 43 measurement planes in 90 minutes. The 0.5-mm fiber bundles viewed a 229-x 229-mm area within the laser light sheet using 4-mm diameter lenses for light collection. The three component fiber bundles were placed adjacent to the multimode fiber (used to transmit a portion of the laser beam), to form an image plane that was viewed by a single DGV receiver system. New and modified procedures needed to accurately measure supersonic flows with fiber-optic based DGV were described. These new and modified procedures were applied with normal DGV operation / data processing procedures to yield single pixel accuracies estimated to be ± 2 m/s based on spatial and temporal standard deviations. The ability of DGV technology to measure flow velocity from 0.1-micron diameter condensation particles makes the technique desirable for supersonic flow field investigations.

References

Clancy, P.; Kim, J.-H.; and Samimy, M. [1996]: *Planar Doppler Velocimetry in High Speed Flows*. AIAA 27th Fluid Dynamics Conference, Paper AIAA 96-1990, New Orleans, LA, June 17-20, 1996.

Clancy, P.; Samimy, M.; and Erskine, W. R. [1998]: *Planar Doppler Velocimetry: Three-Component Velocimetry in Supersonic Jets*. AIAA 36th Aerospace Sciences Meeting & Exhibit, Paper AIAA 98-0506, Reno, NV, January 12-15, 1998.

Dibble, R. W.; Barlow, R. S.; Mungal, M. G.; Lyons, K.; Yip, B.; and Long, M. B. [1989]: *Use of Rayleigh Scattering from Condensed Water Vapor as a Means of Imaging an Underexpanded Supersonic Jet*. STAR Mtg., Nashville, TN, 1989.

Elliott, G. S.; and Beutner, T. J. [1999]: *Molecular Filter Based Planar Doppler Velocimetry*. Progress in Aerospace Sciences, vol. 35, 799-845, 1999.

Elliott, G. S.; Samimy, M.; and Arnette, S. A. [1993]: *Molecular Filter-Based Diagnostics in High Speed Flows*. AIAA 31st Aerospace Sciences Meeting & Exhibit, Paper 93-0512, Reno, NV, January 11-14, 1993.

Elliott, G. S.; Mosedale, A.; Gruber, M. R.; Nejad, A. S.; and Carter, C. D. [1997]: *The Study of a Transverse Jet in a Supersonic Cross-Flow Using Molecular Filter Based Diagnostics*. 33rd AIAA/ASME/SAE/ASEE Joint Propulsion Conference and Exhibit, Paper 97-2999, Seattle, WA, July 6-9, 1997.

Elliott, G. S.; Beutner, T. J.; and Carter, C. D. [2000]: *Application of Planar Doppler Velocimetry Wind Tunnel Testing*. AIAA 38th Aerospace Sciences Meeting & Exhibit, Paper AIAA-2000-0412, Reno, NV, January 10-13, 2000.

Forkey, J. N.; Finkelstein, N. D.; Lempert, W. R.; and Miles, R. B. [1995]: *Control of Experimental Uncertainties in Filtered Rayleigh Scattering Measurements*. AIAA 33rd Aerospace Sciences Meeting & Exhibit, Paper 95-0298, Reno, NV, January 1995.

Komine, H.; Brosnan, S. J.; Litton, A. B.; and Stappaerts, E. A. [1991]: *Real-time Doppler global velocimetry*. AIAA 29th Aerospace Sciences Meeting, Paper 91-0337, Reno, NV, January 7-10, 1991.

Lee, J. W.; and Meyers, J. F. [2005]: *Increased Accuracy in Molecular Filter Based Flow Field Diagnostics Through Direct Frequency Calibration Using Optical Modulators*. 43rd AIAA Aerospace Sciences Meeting and Exhibit, Paper 2005-0033, Reno, NV, January 10-13, 2005.

McKenzie, R. L. [1996]: *Measurement Capabilities of Planar Doppler Velocimetry Using Pulsed Lasers*. Applied Optics, vol. 35, 948-964, 1996.

McKenzie, R. L. [1997]: *Planar Doppler Velocimetry Performance in Low-Speed Flows*. AIAA 35th Aerospace Sciences Meeting & Exhibit, Paper 97-0498, Reno, NV, January 1997.

McKenzie, R. L.; and Reinath, M. S. [2000]: *Planar Doppler Velocimetry Capabilities at Low Speeds and Its Application to a Full-Scale Rotor Flow*. 21st AIAA Aerodynamic Measurement Technology and Ground Testing Conference, Paper AIAA 2000-2292, Denver, CO, June 19-22, 2000.

Meyers, J.F. [1993]: *Looking at Extremes with Laser Velocimetry*. Proceedings of the 11th International Invitational Symposium on the Unification of Analytical, Computational, and Experimental Solution Methodologies, pp. 491-516, Danvers, MA, August, 18-20, 1993.

Meyers, J. F. [1995]: *Development of Doppler Global Velocimetry as a Flow Diagnostics Tool*, Measurement in Fluids and Combustion Systems, Special Issue, Measurement Science and Technology, vol 6, no. 6, pp. 769-783, June 1995.

Meyers, J. F. [1996]: *Evolution of Doppler Global Velocimetry Data Processing*. Eighth International Symposium on Applications of Laser Techniques to Fluid Mechanics, Paper 11.1, Lisbon, Portugal, July 8-11, 1996.

Meyers, J. F., and Lee, J. W. [1999]: *Investigation of Measurement Errors in Doppler Global Velocimetry*. SAE World Aviation Congress and Exposition, Paper 1999-01-5599, San Francisco, CA, October 19-21, 1999.

Meyers, J. F.; Lee, J. W.; Fletcher, M. T.; and South, B. W. [1998]: *Hardening Doppler Global Velocimetry Systems for Large Wind Tunnel Applications*. 20th AIAA Advanced Measurement and Ground Testing Technology Conference, Paper 98-2606, June 15-18, 1998.

Meyers, J. F.; Lee, J. W.; and Schwartz, R. J. [2001]: *Characterization of Measurement Error Sources in Doppler Global Velocimetry*. Measurement Science and Technology, vol. 12, no. 4, pp. 357-368, April 2001.

Naylor, S.; and Kuhlman, J. [1998]: *Accuracy Studies of a Two-Component Doppler Global Velocimeter*. AIAA 36th Aerospace Sciences Meeting & Exhibit, Paper 98-0508, Reno, NV, January 12-15, 1998.

Nobes, D. S.; Ford, H. D.; and Tatam, R. P. [2002]: *Three dimensional planar Doppler velocimetry using imaging fibre bundles*. 40th AIAA Aerospace Sciences Meeting & Exhibit, Paper 2002-0692, Reno, NV, January 14-17, 2002.

Röhle, I. [1999]: *Laser Doppler Velocimetry auf der basis Frequenzselektiver absorption: Aufbau und Einsatz eines Doppler Global Velocimeters*, DLR-Forschungsbericht (DLR reasaerch report), FB 1999-40, 1999.

Röhle, I., and Schodl, R. [1994]: *Evaluation of the Accuracy of the Doppler Global Technique*. Proceeding, Optical Methods and Data Processing in Heat and Fluid Flow, London, pp. 155-161, April 14-15, 1994.

Röhle, I., and Schodl, R. [1997]: *Applications of Three Dimensional Doppler Global Velocimetry to Turbo Machinery and Wind Tunnel Flows*. Proceeding, 7th Intl. Conf. On Laser Anemometry Advances and Applications, Karlsruhe, pp. 387-395, Germany, 1997.

Samimy, M.; and Wernet, M. [2000]: *A Review of Planar Multiple-Component Velocimetry in High Speed Flows*. AIAA Journal, vol. 38, no. 4, April 2000.

Smith, M. W. [1998]: *Application of a planar Doppler velocimetry system to a high Reynolds number compressible jet*. AIAA 36th Aerospace Sciences Meeting & Exhibit, Paper AIAA 98-0428, Reno, NV, January 12-15, 1998.

Smith, M. W.; and Northam, G. B. [1995]: *Application of Absorption Filter Planar Doppler Velocimetry to Sonic and Supersonic Jets*. AIAA 33rd Aerospace Sciences Meeting & Exhibit, Paper AIAA 95-0299, Reno, NV, January 9-12, 1995.

Smith, M. W.; Northam, G. B.; and Dummond, J. P. [1996]: *Application of absorption filter planar Doppler velocimetry to sonic and supersonic jets*. AIAA Journal, vol. 34, 434-441, 1996.

Willert, C.; Stockhausen, G.; Klinner, J.; Beversdorff, M.; Quest, J.; Jansen, U.; and Raffel, M. [2003]: *On the development of Doppler global velocimetry for cryogenic wind tunnels*. IEEE 10th International Congress on Instrumentation in Aerospace Simulation Facilities (ICIASF), Göttingen, Germany, August 25-29, 2003.

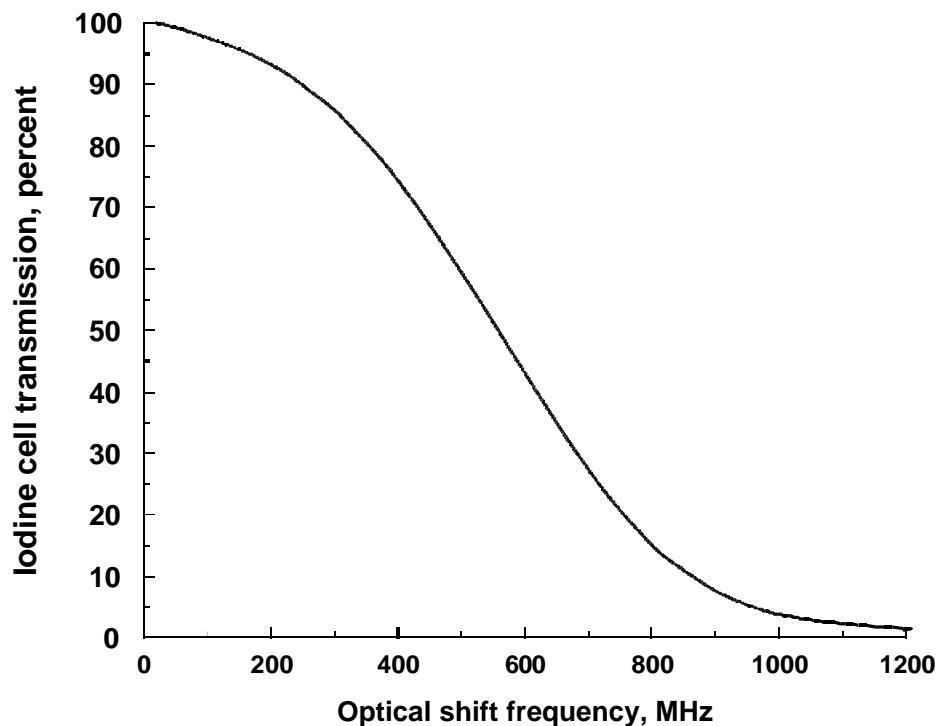


Figure 1. – Iodine vapor cell calibration – DGV measurements of a rotating wheel.

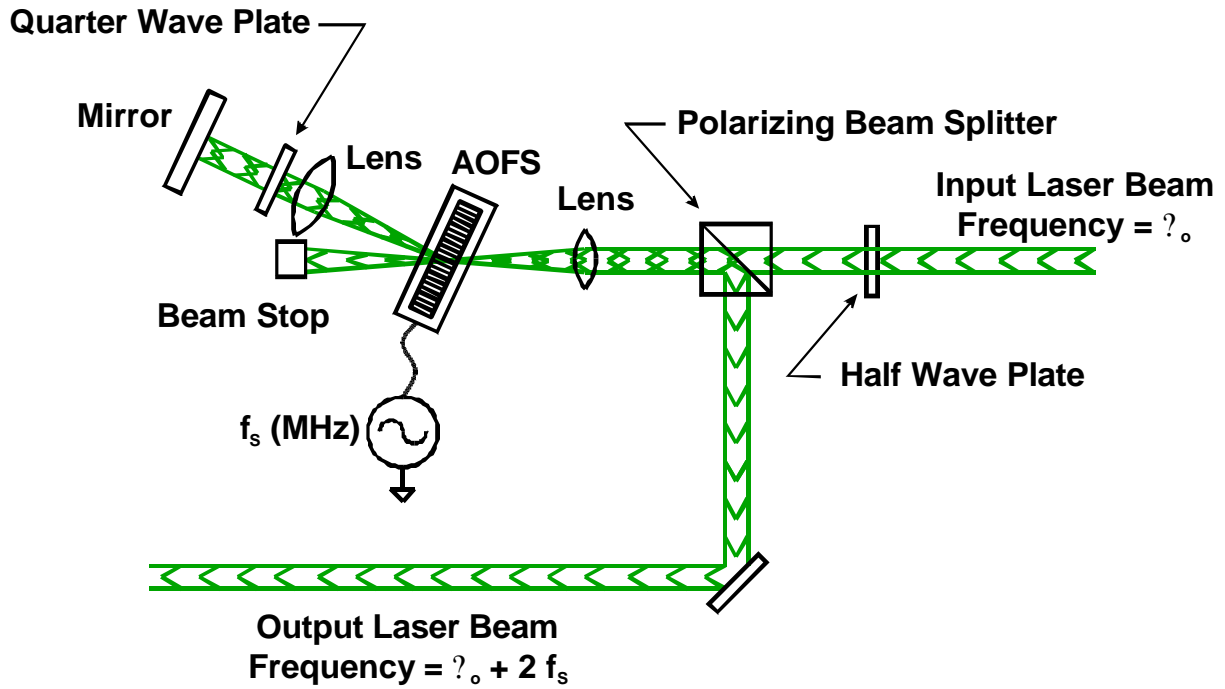


Figure 2. - Schematic of a dual-pass optical configuration for the Acoustic Optic Frequency Shifter.

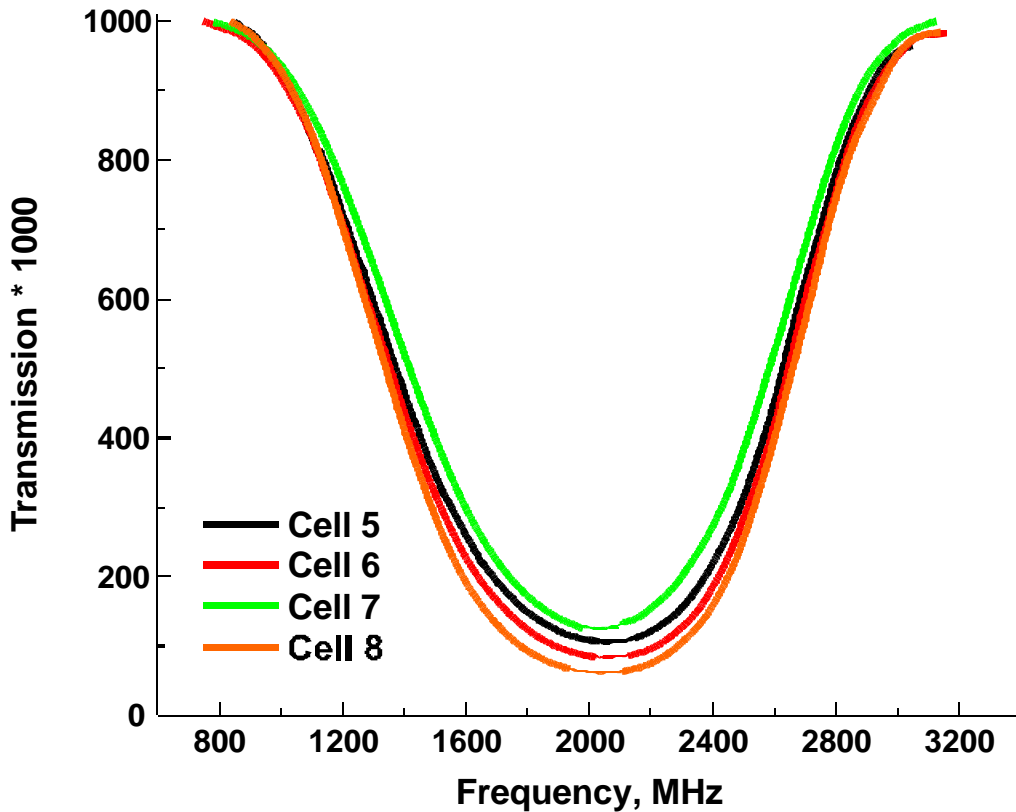


Figure 3. - Iodine vapor cell transfer functions - AOFS based.

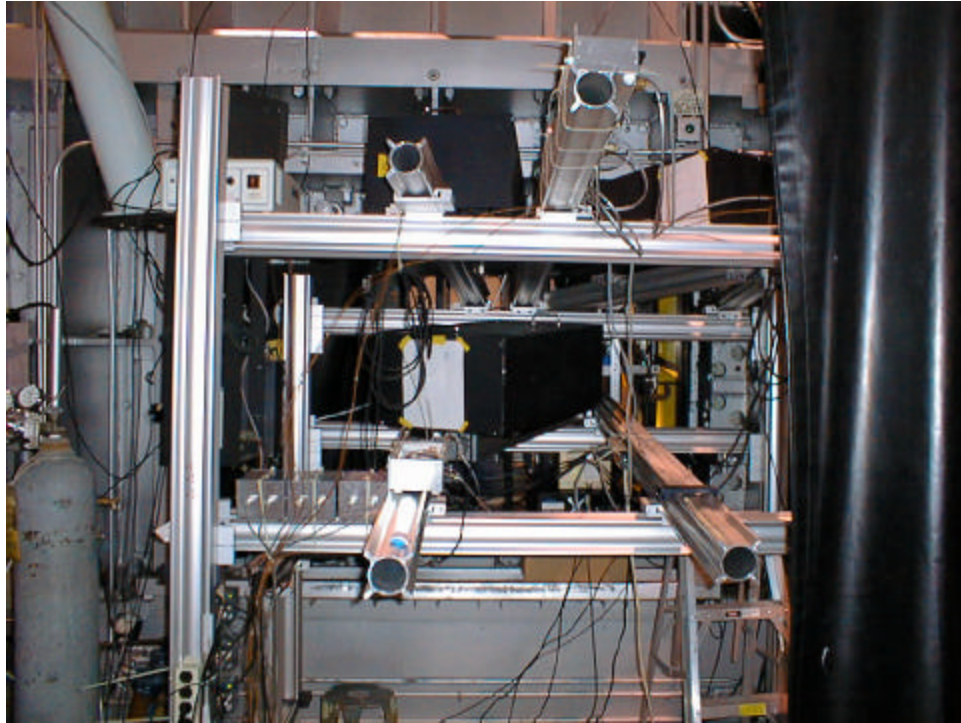


Figure 4. – Installation of a free-space DGV system in the Langley Unitary Plan Wind Tunnel (three receiver system).

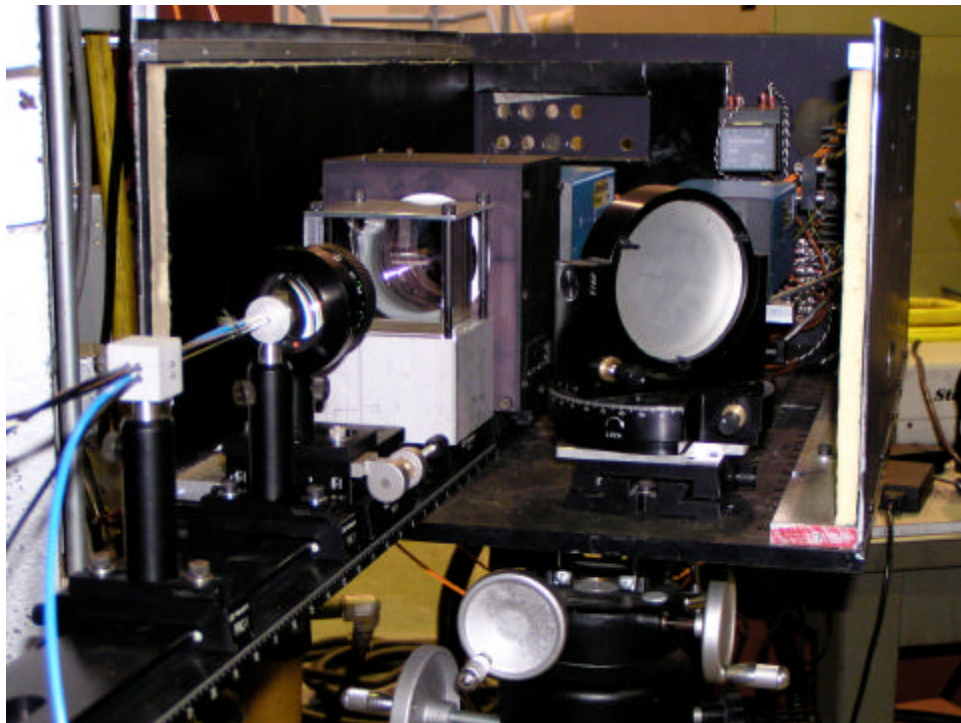


Figure 5. – Fiber optic bundles and image transfer optics to the DGV receiver.

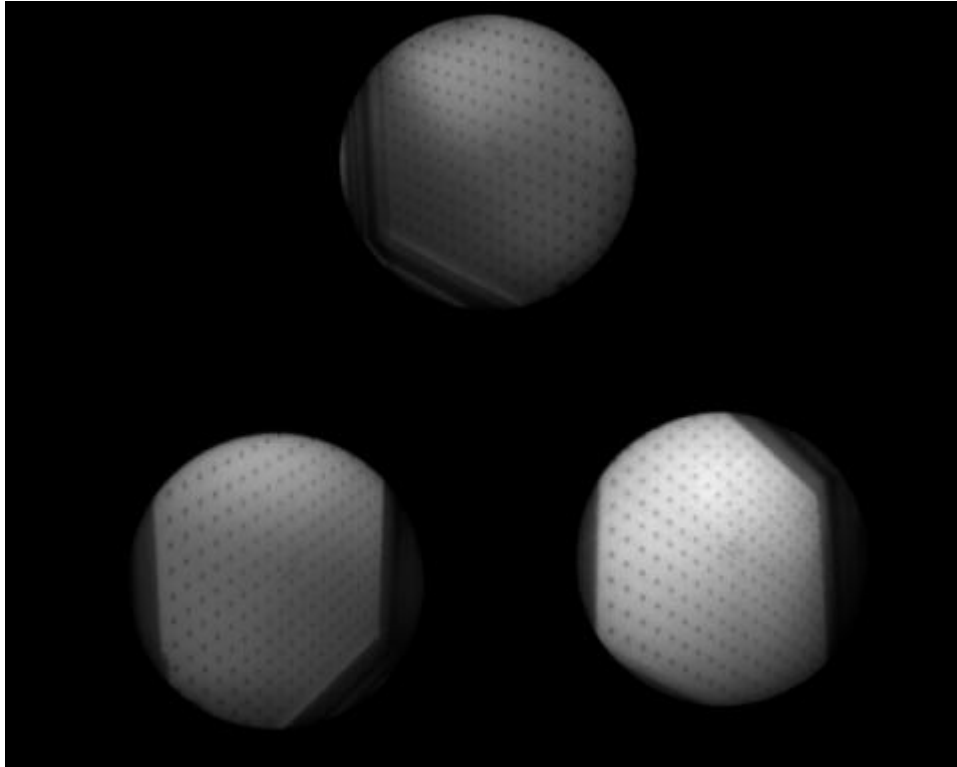
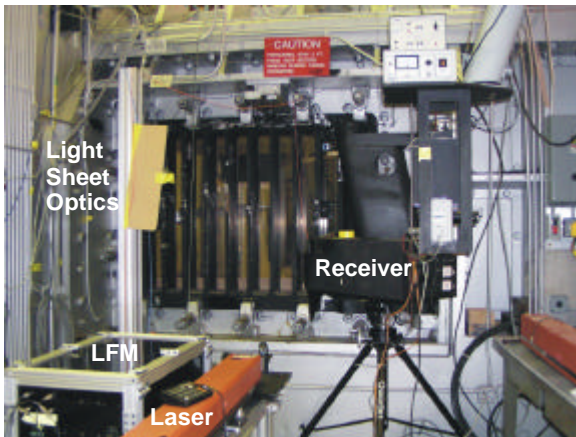
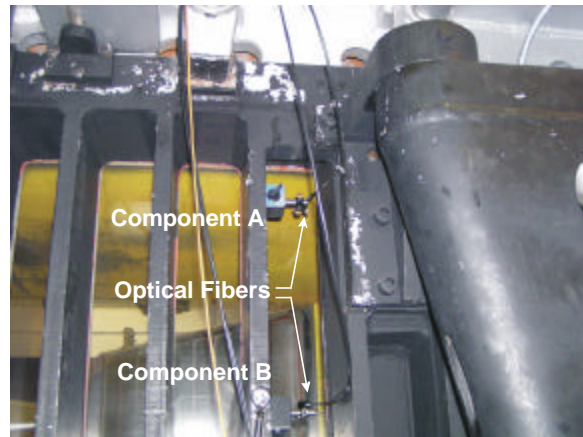


Figure 6. – Registration target as viewed by the three fiber optic bundles.



Doppler Global Velocimeter



Fiber-optic viewing system

Figure 7. – Installation of a fiber-optic based DGV system in the Langley Unitary Plan Wind Tunnel (one receiver system).

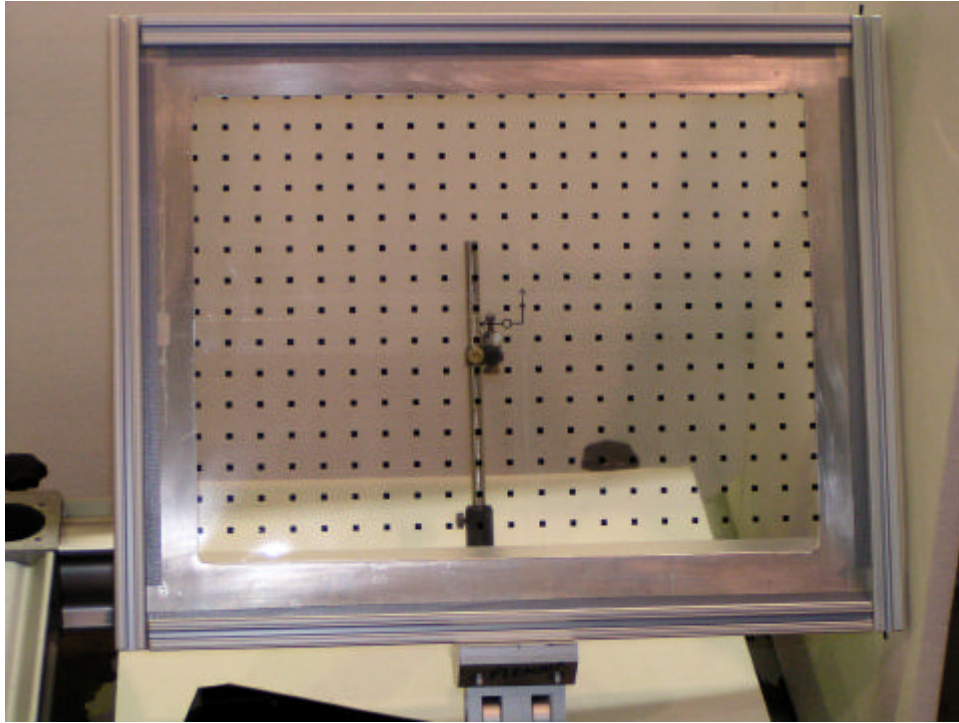
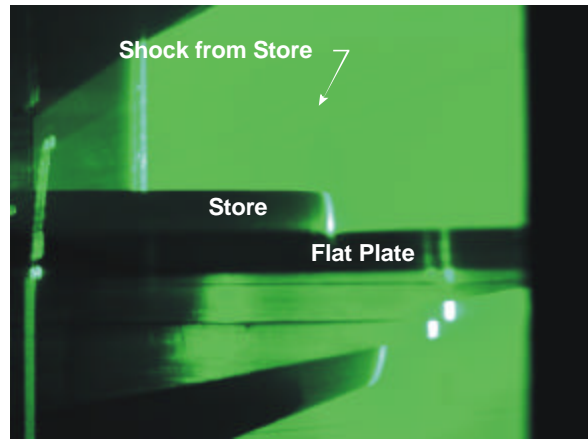


Figure 8. – Registration target set orthogonal to the fiber optic bundle optical axis.



Flat Plate Model with Attached Store



Laser Light Sheet Visualization

Figure 9. – Flat plate model with attached store.

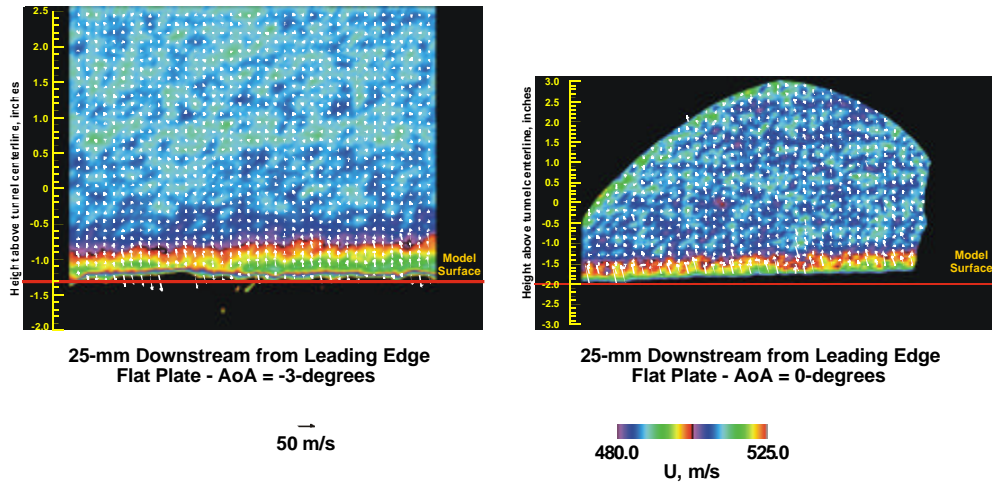


Figure 10.(a) – Flat plate leading edge shock – 25 mm downstream.

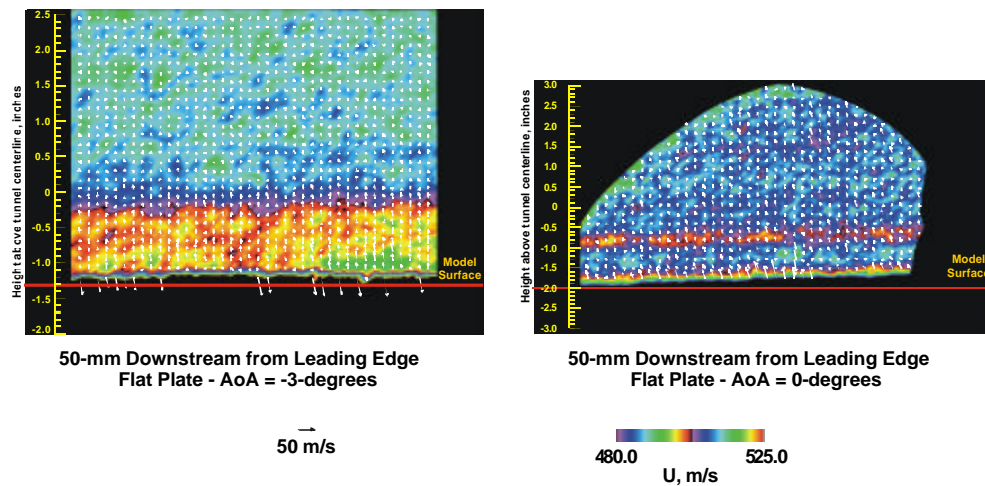


Figure 10.(b) – Flat plate leading edge shock – 50 mm downstream.

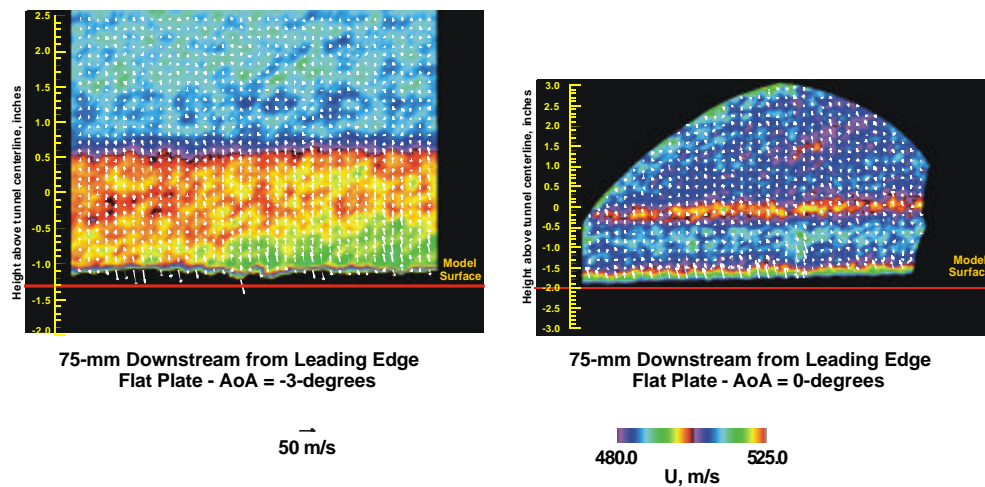


Figure 10.(c) – Flat plate leading edge shock – 75 mm downstream.

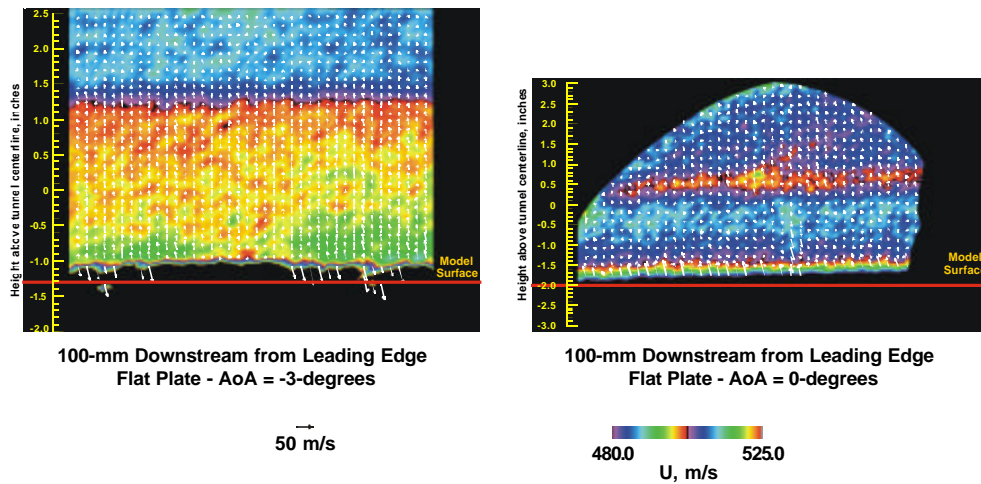


Figure 10.(d) – Flat plate leading edge shock – 100 mm downstream.

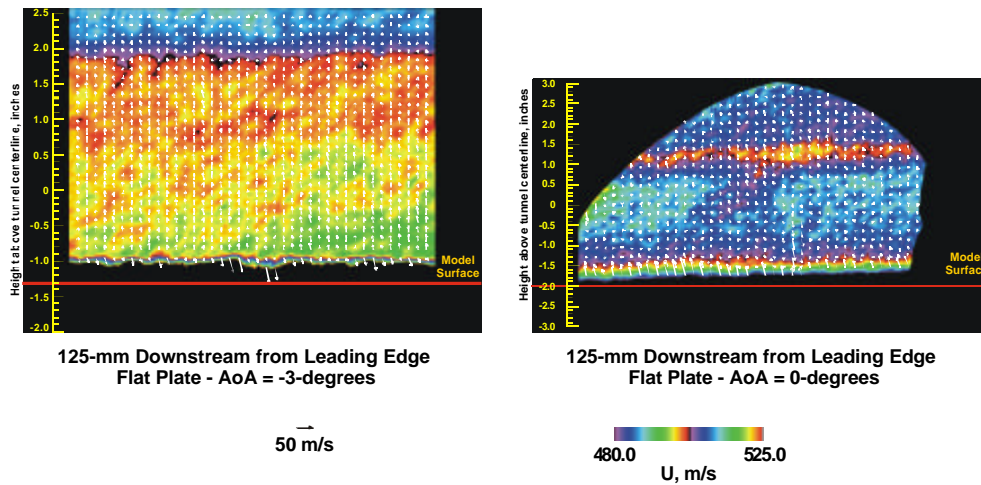


Figure 10.(e) – Flat plate leading edge shock – 125 mm downstream.

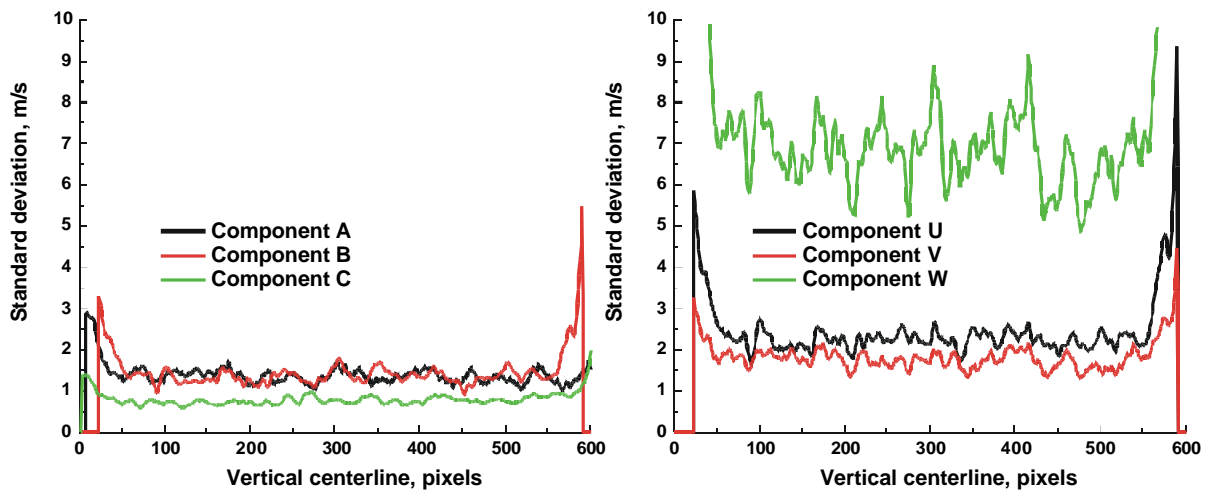


Figure 11. – Temporal standard deviation – 125-mm downstream, AoA = 0 degrees

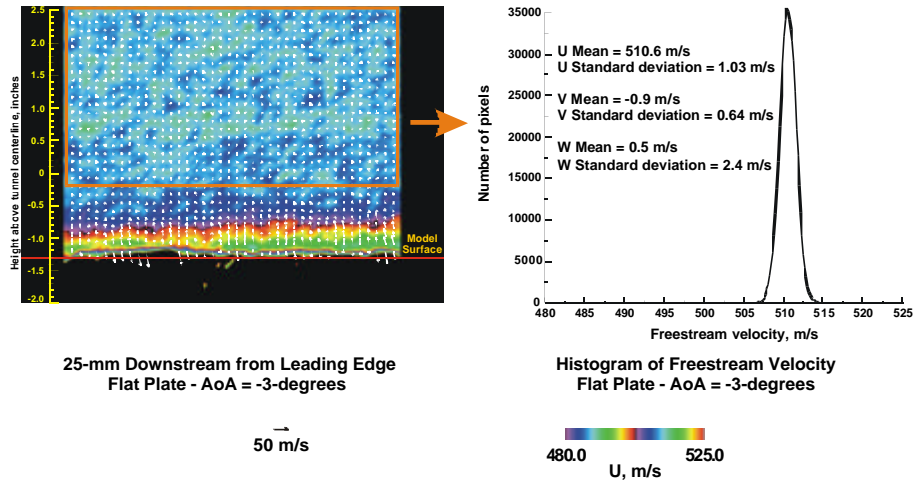


Figure 12. - Spatial standard deviation - 25-mm downstream, AoA = -3 degrees.

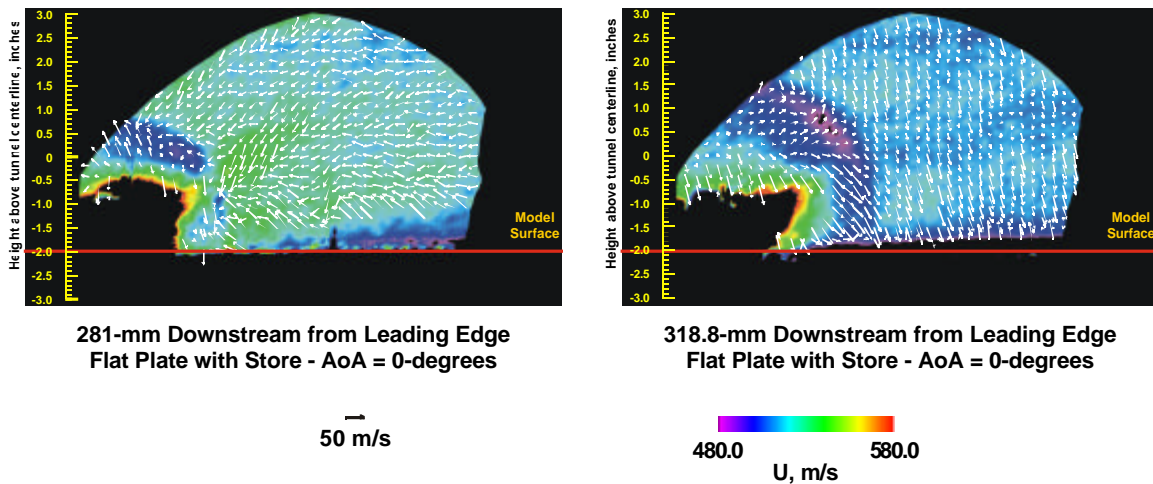


Figure 13.(a) - Flow field about the attached store.

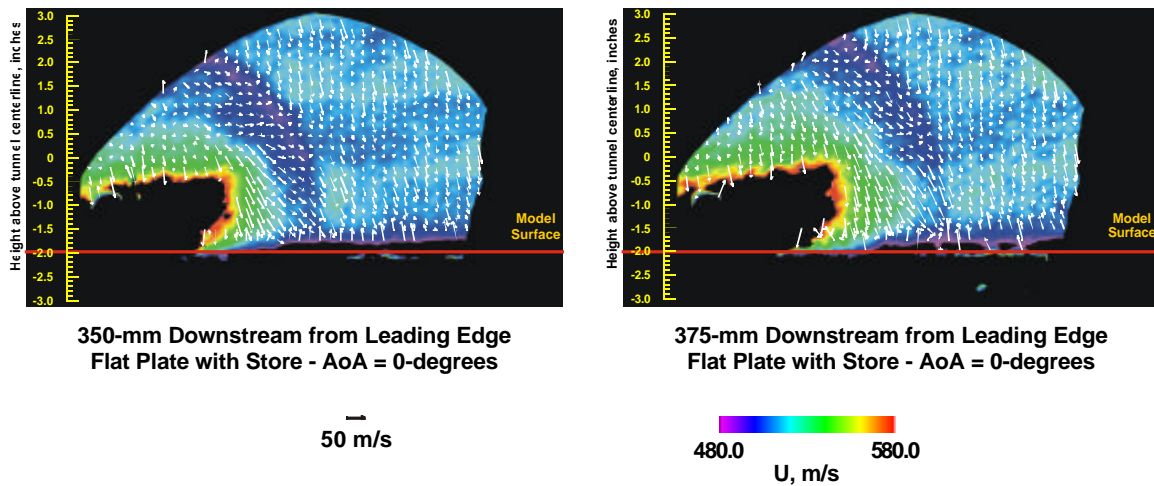


Figure 13.(b) - Flow field about the attached store.

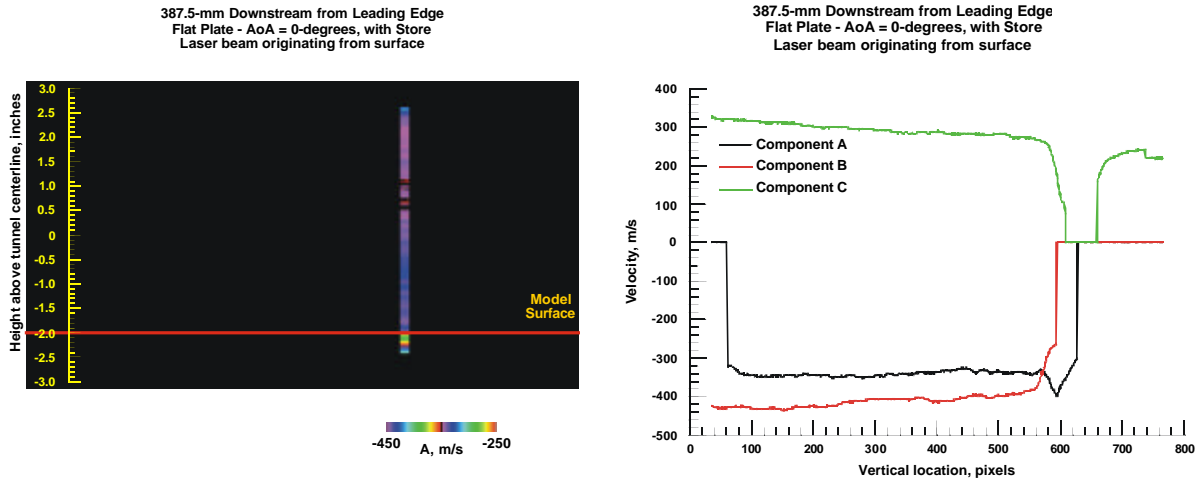


Figure 14. – Boundary layer measurements using a projected laser beam.

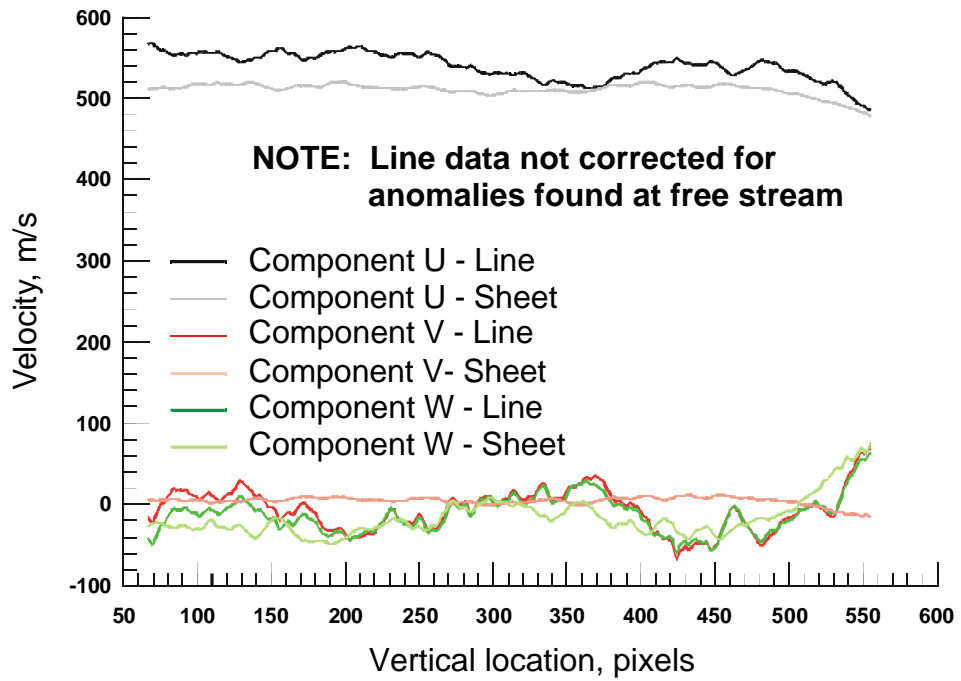


Figure 15. – Comparison of projected beam and light sheet measurements.